

PAPER

Double link sensor for mitigating tilt- horizontal coupling

To cite this article: V. G Nair and C. Collette 2022 *JINST* 17 P04012

View the [article online](#) for updates and enhancements.

You may also like

- [Laser induced fluorescence of cervical tissues: an *in-vitro* study for the diagnosis of cervical cancer from the cervicitis](#)
Ajaya Kumar Barik, Sanoop Pavithran M, Mithun N et al.
- [Self-Consolidating Paving Grade Geopolymer Concrete](#)
M G Girish, Kiran K Shetty and A Rao Raja
- [Morphology, electrical and magnetic study of -Fe₂O₃ coated carbon fabric](#)
R B Jagadeesh Chandra, M Sathish Kumar, B Shivamurthy et al.



ECS The Electrochemical Society
Advancing solid state & electrochemical science & technology

242nd ECS Meeting

Oct 9 – 13, 2022 • Atlanta, GA, US

Presenting more than 2,400 technical abstracts in 50 symposia

  **ECS Plenary Lecture featuring M. Stanley Whittingham, Binghamton University Nobel Laureate – 2019 Nobel Prize in Chemistry**

 **Register now!**



Double link sensor for mitigating tilt- horizontal coupling

V. G Nair^{a,*} and C. Collette^{b,c}

^a*Department of Aeronautical and Automobile Engineering,
Manipal Institute of Technology, Manipal Academy of Higher Education,
Manipal, Karnataka, 576104, India*

^b*Precision Mechatronics Laboratory, Université Libre de Bruxelles,
Bruxelles, Belgium*

^c*Precision Mechatronics Laboratory, Université de Liège,
Liège, Belgium*

E-mail: vishnu.nair@manipal.edu

ABSTRACT: The sensitivity of inertial sensors, intended for horizontal motion detection, to tilt due to gravity at low frequency is known as tilt horizontal coupling. This is crucial for numerous seismological studies and seismic isolation applications such as gravitational wave detection. This paper presents a new sensor architecture for mitigating tilt horizontal coupling when exposed to pure translation or tilt. The proposed Double Link (DL) sensor does not need any additional mechanisms and is only sensitive to the translation and negligibly sensitive to tilt. The sensor is in the form of a double pendulum hanging from a platform and the measured output is the relative motion between the two links. The simulations are carried out in Simscape environment and the results confirms the efficiency of the system. The study was carried out as a part of the ETEST project which is aimed at developing a prototype for the future Einstein Telescope Gravitational Wave detector.

KEYWORDS: Overall mechanics design (support structures and materials, vibration analysis etc); Instrument optimisation; Special materials for GW detectors; Control systems

*Corresponding author.

Contents

1	Introduction	1
1.1	Mathematical model of an inertial sensor	1
1.2	Performance analysis	3
1.2.1	Sensor response to pure translation or tilt	3
2	Related literature	4
3	The proposed double link sensor	7
3.1	Equations of motion	7
3.1.1	Translation	7
3.1.2	Tilt	9
4	Results and discussions	10
4.1	Sensor response to pure translation or tilt	10
4.2	Equilibrated bar configuration	11
5	Conclusion	13

1 Introduction

The sensitivity of horizontal inertial sensors to tilt due to gravity at low frequency, known as tilt horizontal (TH) coupling is a major issue in the field of seismic isolation [1–4]. This is due to the fact that the acceleration sensor alone cannot distinguish the two sources of acceleration — acceleration from horizontal translation or rotation. Normal tiltmeters also have this issue since they gauge tilt by comparing horizontal acceleration to the vertical (at frequencies below their resonances) [5].

1.1 Mathematical model of an inertial sensor

The inertial sensor basically consists of an inertial mass, whose relative motion due to the displacement of the platform on which it is fixed, gives the absolute measurement. All inertial sensors can be modeled as a simple linear time-invariant (LTI) spring-mass system with damping. A schematic of general inertial sensor is given in figure 1. The M is the inertial mass, y is the relative displacement between the inertial mass and the support, k is the spring stiffness, c is the damping coefficient, x is the displacement of the mass and w is the absolute displacement of the ground.

The dynamics equation of the mass is given by,

$$M\ddot{x} + c(\dot{x} - \dot{w}) + k(x - w) = -Mg \quad (1.1)$$

Where g is the acceleration due to gravity.

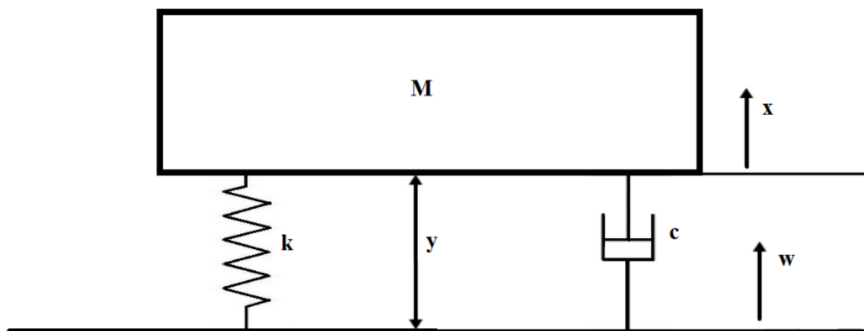


Figure 1. Schematic of an inertial sensor.

Considering zero initial condition and rewriting the equation as a function of y , the Laplace transform will be

$$Ms^2Y + csY + kY = -Ms^2W \quad (1.2)$$

From the above equation, the transmissibility between the displacement of the attachment point $W(s)$ and the relative displacement $Y(s)$ is given by

$$T_{wy}(s) = \frac{Y(s)}{W(s)} = \frac{-Ms^2}{Ms^2 + cs + k} \quad (1.3)$$

It is noted that at frequencies above resonances, the measurement of $Y(s)$ is a perfect estimator for $W(s)$ [6].

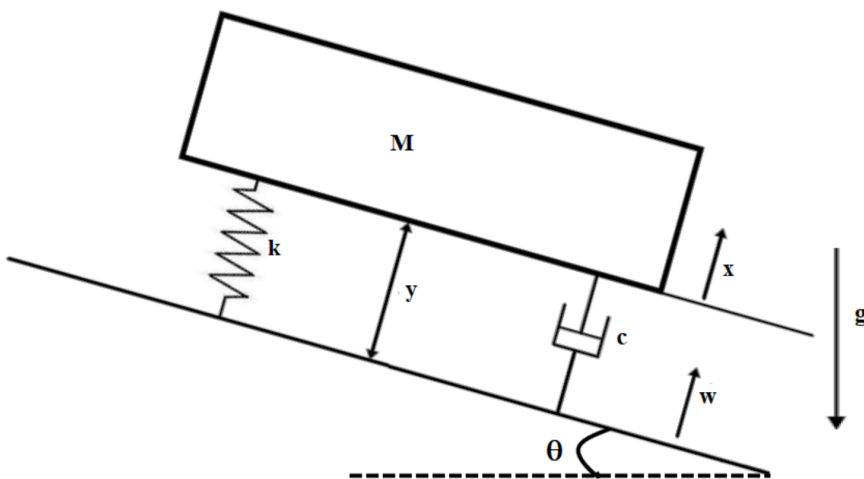


Figure 2. Tilted inertial sensor.

If we include tilt (as shown in the figure 2) in the inertial sensor dynamics which is explained above the equation will be modified as below [6].

$$M\ddot{x} + c(\dot{x} - \dot{w}) + k(x - w) = -Mg \cos \theta \quad (1.4)$$

Linearizing the equation around a nominal angle θ_0 and choosing zero initial conditions, in the Laplace domain we obtain,

$$Y(s) = \frac{-Ms^2}{Ms^2 + cs + k}W(s) - \frac{Mg \sin \theta_0}{Ms^2 + cs + k}\theta(s) \quad (1.5)$$

where θ is the tilt angle.

The above equation infers that an inertial sensor cannot distinguish between a displacement of the support and a modification of the orientation with respect to the gravitational field. The coupling is maximum for $\theta_0 = \pi/2$ and is known as tilt-to-horizontal coupling.

1.2 Performance analysis

In this section, an inertial sensor is modelled in Simscape and is simulated for various scenarios. The sensor is mounted on a platform and two configurations are presented, one with the sensor mounted on a platform in which the input is the forces applied to the platform (pure translation or tilt) and the other one in which the platform is fixed to the ground using springs and the input signal is the ground motion. The results of both configurations are presented and it is inferred that the TH coupling plays a vital role in the sensor performance as explained in the above sections.

1.2.1 Sensor response to pure translation or tilt

The sensor is in the form of a horizontal pendulum with inertial mass, M , fixed on a platform (Shaded/Green rectangle). The y axis is the horizontal axis, z axis is the vertical. The link L is connected to the platform via a rotating joint R and can be displaced in x direction by moving the platform in x . The sensor responses, $\frac{Y(s)}{W(s)}$ and $\frac{Y(s)}{\theta(s)}$ is taken for the translation of the platform in x direction (W_x) and tilt about y axis (θ_y) (figure 3).

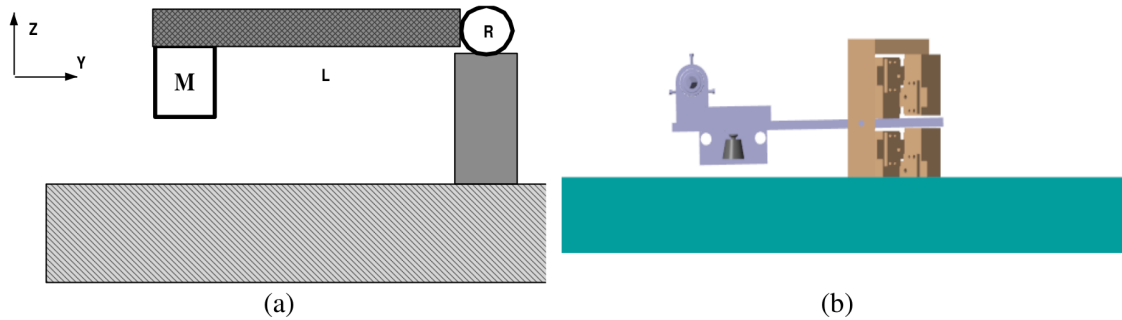


Figure 3. Inertial sensor on a platform (a) Schematic (b) Simscape model. The sensor is in the form of a horizontal pendulum with inertial mass, M , fixed on a platform (Shaded/Green rectangle). The link L is connected to the platform via a rotating joint R and can be displaced in x direction by moving the platform in x . The sensor responses are taken for the translation of the platform in x (W_x) direction and tilt about y axis (θ_y).

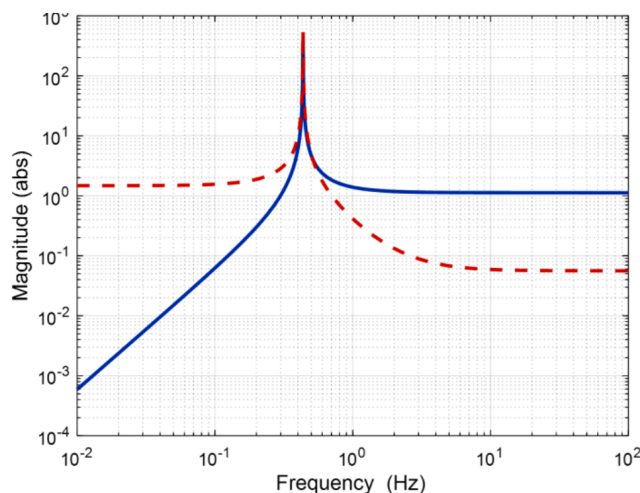
Figure 4 shows the response of the sensor to the translation and tilt of the platform. The values considered for the simulations are in table 1.

As expected, the sensor is sensitive to both translation and tilt. The coupling is more pronounced at lower frequencies which makes such sensors inefficient for low frequency operations such as

Table 1. The values considered for the simulation.

Parameter	Value
Length of the pendulum	10 cm
Stiffness of joint	0.1 N*m/rad
Mass of the pendulum	200 g

Gravitational Wave Detectors. Below the natural frequency from 4.4×10^{-1} Hz, the magnitude of the tilt response remains almost constant (3.36 dB) while that of the translation falls from 0.162 dB at 2.9×10^{-1} Hz to -64.3 dB at 10^{-2} Hz. Overall, it can be observed that the magnitude of the tilt increases as the frequency decreases, up to the natural frequency of the system, at which point it becomes constant. The translation response is constant above the natural frequency, but begins to fall off below this frequency.

**Figure 4.** Response of the sensor to translation $\frac{Y(s)}{W(s)}$ (blue/bold) and tilt $\frac{Y(s)}{\theta(s)}$ (red/dotted).

2 Related literature

In order to minimize the problem of TH coupling various schemes are available in literature. Fabrice Matichard et al. [7] has given a fantastic review on TH coupling and various methods proposed/implemented for its removal. The authors also analyse the limitations of each of these methods related to sensor noise and geometrical couplings. Collette [6] has given an informative review on inertial sensors and also discussed briefly about TH coupling. In LIGO VIRGO collaboration, two approaches are being studied for eliminating the TH coupling. The first one is to develop a seismometer that is insensitive to tilt in a particular frequency band [7, 8]. The second aims to actively stabilize the tilt-motion of the isolated platforms using 1D rotation sensors. In [9], the authors presented a patented scheme to eliminate TH coupling. In this method, the absolute inertial sensor is attached to the floor with a fixation that is rigid only in the tilting direction and

very compliant for the other five degrees of freedom. Wensheng Hua [10], in his doctoral thesis, presented optimal FIR complementary filters to separate tilt motion from horizontal acceleration. Both these methods need an additional systems or structures which makes them inferior to the sensor proposed in this paper. In [11] the authors proposed a novel approach called ‘6D’ which is claimed to have a better isolation between translation and tilt at low frequencies. It is an absolute inertial isolation scheme based on six degree-of-freedom (6D) interferometric readout of a single reference mass. It is a two-stage system in which the reference mass is suspended within the platform to be isolated, which is itself suspended from the ground. The 6D method proved to be an effective one in reducing inertial motion by more than two orders of magnitude at 100mHz but the performance of it with respect to tilt horizontal coupling needs further investigation. The system measures the motion between the payload and the suspended structure, while the DL sensor proposed in this paper measures the relative displacement /rotation between the two suspended links. Both the 6D as well as the DL system has several advantages in comparison with other similar approaches. Both of them require a single device for all degrees of freedom. For example, LIGO uses three 3D Trillium seismometers, six GS-13 geophones, and six L-4C geophones per platform [11]. The proposed DL system can be an extremely cheaper and easy to install device as compared to 6D. Even though no study on the material properties of the DL sensor is carried out, since the performance mostly depends on the link joints (since the output is the relative motion between the links), very low emphasis is needed on the design as compared to 6D. Another method to isolate displacement and rotation is to measure tilt/rotation (with respect to the inertial frame) using beam-balances [12]. This independent sensor can then be used to subtract the tilt component from a seismometer’s output to provide a pure displacement output. If the sensors measure identical signals, the subtraction would be limited only by the noise in the two sensors. However, in practice since the sensors are separated by some distance, the subtraction could be limited by the difference in tilt between the two locations. Mechanical filtering of the tilt transmission to a seismometer is an interesting alternative technique of measuring tilt-free horizontal displacement [13] as compared to direct tilt measurement and subtraction.

Winterflood et al. [14] presented an idea based on this. It is a tilt sensor composed of a bar suspended by a metallic glass flexure with a shadow-sensor readout with a reported sensitivity of $0.2 \text{ nrad}/\sqrt{\text{Hz}}$ above 1 Hz. It is shown that the rms vibration levels in a interferometric gravitational wave detector can be effectively suppressed using a combination of ultra-low frequency vibration isolators and high sensitivity tilt sensing and feedback. Cheng et al. [15] also proposed a similar, but modified one presented above. It presents a double-flexure two-axis tilt sensor with a tilt readout based on an optical walk-off sensor. The walk-off sensor has demonstrated a sensitivity of $10^{-11} \text{ rad Hz}^{-1/2}$ at 1 Hz. The tilt sensor has measured seismic noise $\sim 10^{-9} - 10^{-10} \text{ rad Hz}^{-1/2}$ for frequency in the 2–10 Hz range. In the same measurement band, Allocca et al. [23] performed a direct measurement of seismic noise of order $10^{-12} \text{ rad Hz}^{-1/2}$. Krishna Venkateshwara [5] used rotational sensors to sense and cancel tilt from the translation output. The tilt subtraction is done using a low-frequency beam-balance whose angle is measured using a high-sensitivity autocollimator. Andrew Sunderland et al. [16] presented a rotational vibration isolator which is in the form of a sphere plunged in a liquid. The sensor has an extremely low resonant frequency of $0.055 \pm 0.002 \text{ Hz}$. It consists of two concentric spheres separated by a layer of water and joined by very soft silicone springs so as to achieve softest possible restoring force. The isolator reduces

rotation noise at all frequencies above its resonance. Electromagnetic sensor coils are placed inside the inner sphere. In addition to the above there are various configurations proposed such as liquid interferometric sensors, sensor using Bragg grating optical fibres etc. Matichard and Sohier [17] proposed a suspended seismometer model in which the inertial terms are included. This technique does not require an auxiliary rotation sensor, and can produce a lower noise measurement, while maintaining adequate translation sensitivity and measurement noise in the bandwidth of interest. This method closely resembles the one proposed in this paper but the complexity is more and performance in handling coupling is low as given in figure 13. Philipp Knothe [18] in his master's thesis studied the performance of suspended seismometers. Other than using a suspended seismometer, a highly sensitive one can also be implemented to have a very accurate measurement of ground horizontal motion [19]. A seismometer with that high sensitivity has been designed as an inverted pendulum and a Michelson interferometer readout. The suspended platform, called “rhomboid”, is suspended from above using two thin steel wires attached to an aluminium frame. Placed at the center of mass of the rhomboid is the inverted pendulum. The Michelson interferometer is built on top of the rhomboid and inverted pendulum and it measures the relative distance between these two. From this measurement we can extract the spectrum of ground motion. All the above methods have some or the other drawbacks such as addition of extra mechanisms or sensors, noise etc.

A decoupling efficiency ratio, $R = \frac{Y(s)}{\theta(s)} / \frac{Y(s)}{W(s)}$, for the suspended seismometer and regular inertial sensor configuration shown in figure 3 is given in figure 5. The ratio represents the effectiveness of a sensor to handle TH coupling. The smaller the value, the higher will be the decoupling capability of the sensor. For the inertial sensor configuration, the value of R is high which is also a clear indication of its inability to handle TH coupling. This paper presents a simple sensor architecture which outperforms all these and is capable of mitigating the TH coupling at almost all frequencies.

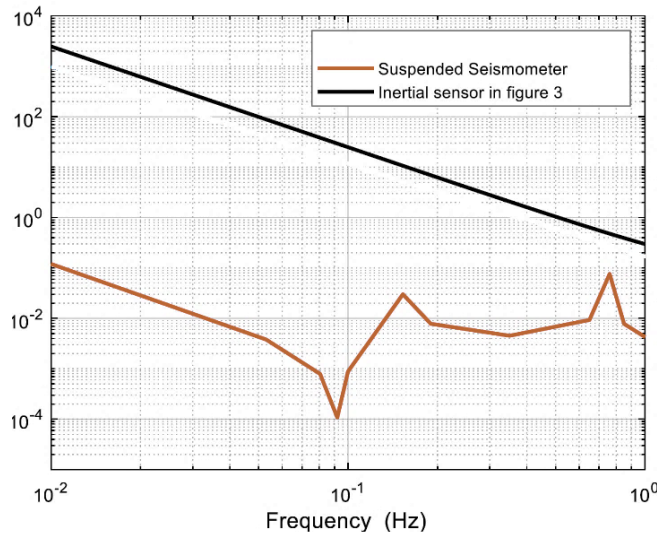


Figure 5. Comparison of tilt to translation ratio, R , for suspended seismometer and regular inertial sensor configuration.

3 The proposed double link sensor

A sensor which is capable of mitigating the TH coupling is proposed in this paper. The sensor consists of two links like a double pendulum system, attached with the platform using negligible stiffness joints. A frictionless scenario is considered. The relative motion between the links is the output of the sensor. When the platform translates the sensor will provide a significant output but when it tilts the output is low since the relative motion is negligible. Thus, the sensor is sensitive only to translation and negligibly sensitive to tilt (figure 6). Such a sensor is capable of mitigating TH coupling especially at low frequencies and is a good candidate for the such applications.

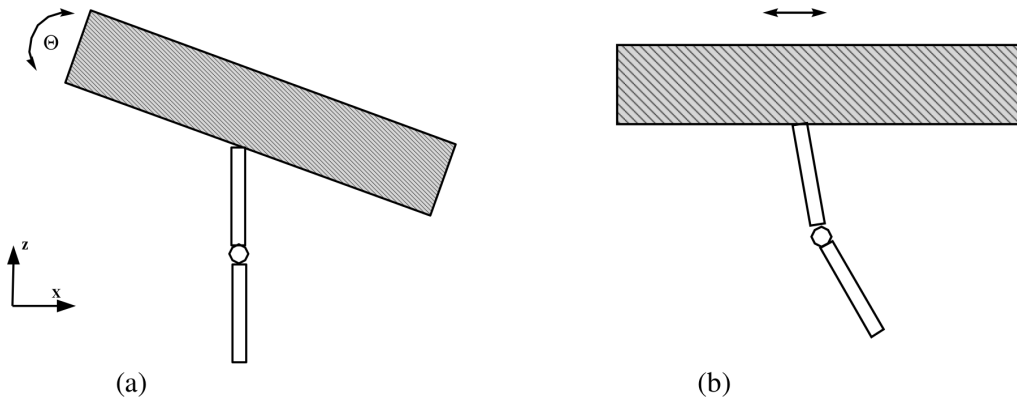


Figure 6. Response of the double pendulum sensor to (a) Tilt and (b) Translation. The relative motion between the links are prominent in the case of translation and negligible during tilt.

3.1 Equations of motion

The Equations of Motion (EOM) of the system can be found by various methods, including Newton’s laws and the Lagrange method. Lagrange method is followed in this paper. The following sections provides an insight into the development of EOM for the translation as well as the tilt inputs.

3.1.1 Translation

Figure 7 shows the schematic used for the derivation of the EOM of the sensor when the platform of mass M_p is translated in x direction (x_p) by a force F_x . L_1 and L_2 are the lengths of the two links of the pendulum with masses M_1 and M_2 respectively. θ_1 and θ_2 are the angles made by the links L_1 and L_2 with vertical. The output of the sensor is $\theta_d = \theta_1 - \theta_2$. Since the motion of the links is imposed by the platform, its dynamics is not considered for the derivation.

For Link, L_1 .

$$\text{Kinetic Energy,} \quad KE_1 = \frac{M_1}{2} (\dot{x}_p)^2 + \frac{M_1}{2} (L_1 \dot{\theta}_1)^2 + M_1 \dot{\theta}_1 L_1 \dot{x}_p \cos \theta_1 \quad (3.1)$$

$$\text{Potential Energy,} \quad PE_1 = -M_1 g L_1 \cos \theta_1 + \frac{1}{2} k_1 \theta_1^2 \quad (3.2)$$

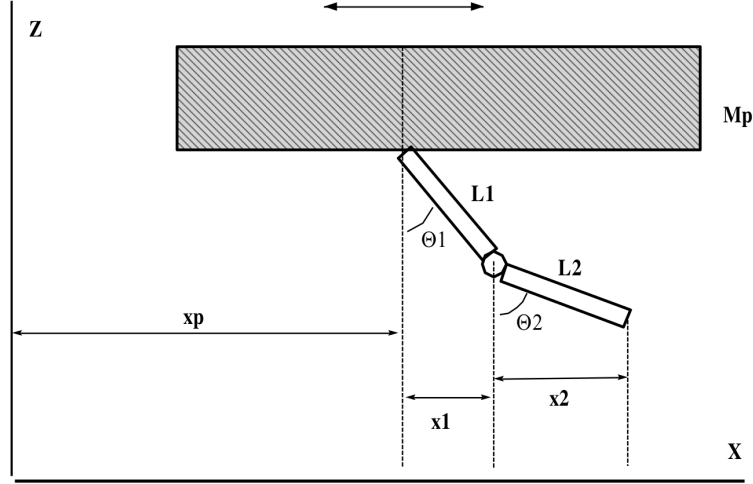


Figure 7. The schematic used for the derivation of equations of motion for translation.

For Link, L_2 .

$$\begin{aligned} \text{Kinetic Energy, } KE_2 &= \frac{M_2}{2} (\dot{x}_p)^2 + \frac{M_2}{2} (L_1 \dot{\theta}_1)^2 + \frac{M_2}{2} (L_2 \dot{\theta}_2)^2 \\ &\quad + M_2 \dot{\theta}_1 \dot{\theta}_2 L_1 L_2 \cos(\theta_1 - \theta_2) + M_2 \dot{x}_p \dot{\theta}_1 L_1 \cos \theta_1 \\ &\quad + M_2 \dot{x}_p \dot{\theta}_2 L_2 \cos \theta_2 \end{aligned} \quad (3.3)$$

$$\text{Potential Energy, } PE_2 = -M_2 g L_1 \cos \theta_1 - M_2 g L_2 \cos \theta_2 + \frac{1}{2} k_2 \theta_2^2 \quad (3.4)$$

Lagrangian.

$$\begin{aligned} L &= \frac{1}{2} M_p \dot{x}_p^2 + \frac{M_1}{2} (\dot{x}_p)^2 + \frac{M_1}{2} (L_1 \dot{\theta}_1)^2 + M_1 \dot{\theta}_1 L_1 \dot{x}_p \cos \theta_1 + \frac{M_2}{2} (\dot{x}_p)^2 + \frac{M_2}{2} (L_1 \dot{\theta}_1)^2 \\ &\quad + \frac{M_2}{2} (L_2 \dot{\theta}_2)^2 + M_2 \dot{\theta}_1 \dot{\theta}_2 L_1 L_2 \cos(\theta_1 - \theta_2) + M_2 \dot{x}_p \dot{\theta}_1 L_1 \cos \theta_1 + M_2 \dot{x}_p \dot{\theta}_2 L_2 \cos \theta_2 \\ &\quad + M_1 g L_1 \cos \theta_1 + M_2 g L_1 \cos \theta_1 + M_2 g L_2 \cos \theta_2 - \frac{1}{2} k_1 \theta_1^2 - \frac{1}{2} k_2 \theta_2^2 \end{aligned} \quad (3.5)$$

Equations of motion: can be now expressed as

$$\frac{d}{dt} \left(\frac{\partial L}{\partial \dot{\theta}_1} \right) - \frac{\partial L}{\partial \theta_1} = F_x \quad (3.6)$$

$$\frac{d}{dt} \left(\frac{\partial L}{\partial \dot{\theta}_2} \right) - \frac{\partial L}{\partial \theta_2} = 0 \quad (3.7)$$

From the above representations, the simplified equation of motion is in the form [22],

$$\begin{aligned} (M_1 + M_2) \left[(L_1 \ddot{\theta}_1 + g \sin \theta_1) \right] + M_2 L_2 \left[(\ddot{\theta}_1 + \ddot{\theta}_2) \cos \theta_2 - (\dot{\theta}_1 + \dot{\theta}_2)^2 \sin \theta_2 \right] \\ - \ddot{x}_p (M_1 + M_2) \cos \theta_1 + k_1 \theta_1 = 0 \end{aligned} \quad (3.8)$$

and

$$L_2 (\ddot{\theta}_1 + \ddot{\theta}_2) + g \sin(\theta_1 + \theta_2) + L_1 \left[\dot{\theta}_1^2 \sin \theta_2 + \ddot{\theta}_1 \cos \theta_2 \right] - \ddot{x}_p \cos(\theta_1 + \theta_2) - k_2 \theta_2 = 0 \quad (3.9)$$

For small values of θ_1 and θ_2 , and simplifying:

$$(M_1 + M_2) (L_1 \ddot{\theta}_1) + M_2 L_2 [(\ddot{\theta}_1 + \ddot{\theta}_2) \theta_2] - \ddot{x}_p (M_1 + M_2) \theta_1 + k_1 \theta_1 - L_2 (\ddot{\theta}_1 + \ddot{\theta}_2) + L_1 [\ddot{\theta}_1 \theta_2] - \ddot{x}_p (\theta_1 + \theta_2) - k_2 \theta_2 = 0 \quad (3.10)$$

Taking Laplace Transform of equation (3.10) and simplifying we get

$$\theta_1(s) [L_1 M_1 s^2 + L_1 M_2 s^2 - M_1 s^2 x_p(s) - M_2 s^2 x_p(s) - L_2 s^2 + s^2 x_p(s) + k_1] + \theta_2(s) [L_2 M_2 s^2 \theta_2(s) - L_2 s^2 + s^2 x_p(s) + k_2] + \theta_1(s) \theta_2(s) [L_2 M_2 s^2 - L_1 s^2] = 0 \quad (3.11)$$

3.1.2 Tilt

Consider the platform is tilted by an angle, γ due to a torque applied about y axis and there is no translation. A highly exaggerated schematic is given in the figure 8. The sensitivity of the proposed sensor to tilt is negligible. So, the angle θ_d will be very small in real scenario. For deriving the dynamics, we will use the Lagrange method as in the case of translation [20].

Following the same procedure as above and assuming $L_1 = L_2 = L$, $M_1 = M_2 = M$ and $\theta_1 - \theta_2 = \theta_d$, the final simplified equation of motion is given in equation (3.12), where k_p is the stiffness of the platform.

$$\ddot{\theta}_d (1 - \tan \theta_d) - \dot{\theta}_d \dot{\theta}_2 \sin \theta_d + \dot{\theta}_1^2 \sin \theta_d - \frac{g}{L} \sin \theta_2 - k_p \gamma - \frac{M_p g L}{2} \sin \gamma = 0 \quad (3.12)$$

For small values of θ_1 , θ_2 and γ the equation (3.12) becomes

$$\ddot{\theta}_d (1 - \theta_d) - k_p \gamma = 0 \quad (3.13)$$

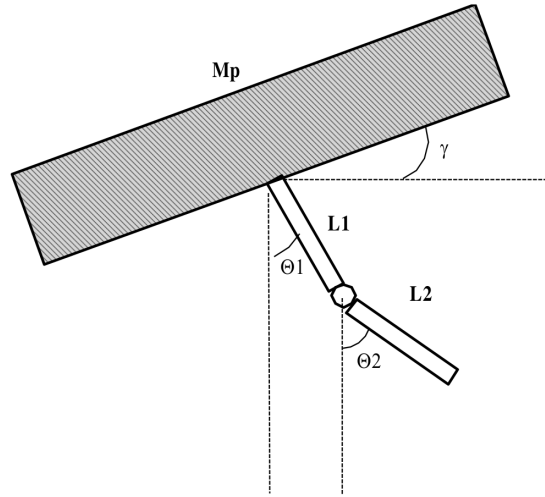


Figure 8. The schematic used for the derivation of equations of motion for tilt.

The expression for decoupling efficiency ratio, R, can be derived from equations (3.11) and (3.12)

$$\frac{s^2(\theta_1(s) - \theta_2(s))[1 - (\theta_1(s) - \theta_2(s))] - k_p \gamma(s)}{\theta_1(s)[L_1 M_1 s^2 + L_1 M_2 s^2 - M_1 s^2 x_p(s) - M_2 s^2 x_p(s) - L_2 s^2 + s^2 x_p(s) + k_1] + \theta_2(s)[L_2 M_2 s^2 \theta_2(s) - L_2 s^2 + s^2 x_p(s) + k_2] + \theta_1(s) \theta_2(s) [L_2 M_2 s^2 - L_1 s^2]} \quad (3.14)$$

4 Results and discussions

The proposed sensor mounted on a platform is modelled in Simscape. The values considered for the simulations are in table 2.

Table 2. The values considered for the simulation.

Parameter	Value
Length of Link 1	10 cm
Length of Link 2	10 cm
Mass of Link 1	200 g
Mass of Link 2	200 g

4.1 Sensor response to pure translation or tilt

The sensor is in the form of a double pendulum with link masses, M_1 and M_2 fixed on a platform (figure 9). The y axis is the horizontal axis, z axis is vertical. The forces applied for the analysis are the translation in x direction and tilt about y axis.

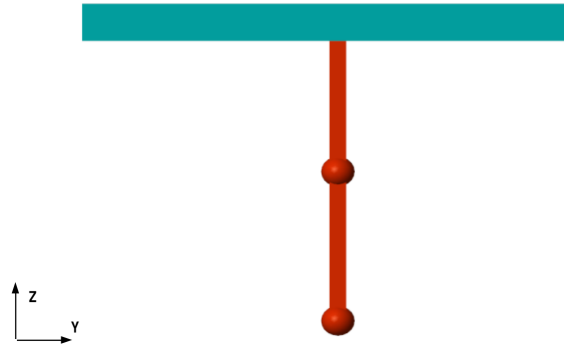


Figure 9. Simscape model of the proposed sensor on a platform. The sensor is in the form of a double pendulum with link masses, M_1 and M_2 , fixed on a platform (Green rectangle). The forces applied for the analysis are the translation in x direction and tilt about y axis.

Figure 10 shows the response of the proposed sensor to the translation in x direction, $\frac{Y_{new}}{W_{new}}$ and tilt about y axis, $\frac{Y_{new}}{\theta_{new}}$ of the platform. The sensor is highly sensitive to translation but very low to tilt. This property makes such sensors efficient for a wide variety of applications where the TH coupling is not acceptable such as Gravitational Wave Detectors. Comparing with the data from the inertial sensor explained in figure 4, above natural frequencies of the links, $\frac{Y_{new}}{W_{new}}$ is almost constant at -3.11 dB and below, the value decreases. Also, $\frac{Y_{new}}{\theta_{new}}$ is almost 10^{10} orders of magnitude below.

Figure 11 shows the effect of various parameters of the sensor on the value of R. It is observed that when the length of link 2 increases the decoupling efficiency is getting better. This is because as the motion of link 2 gets constrained as compared to link 1 as the length increases, when the platform is undergoing a tilt. Link 1 is directly connected to the platform. It's motion, as the platform moves will directly depend on the stiffness of the joint connecting it with the platform.

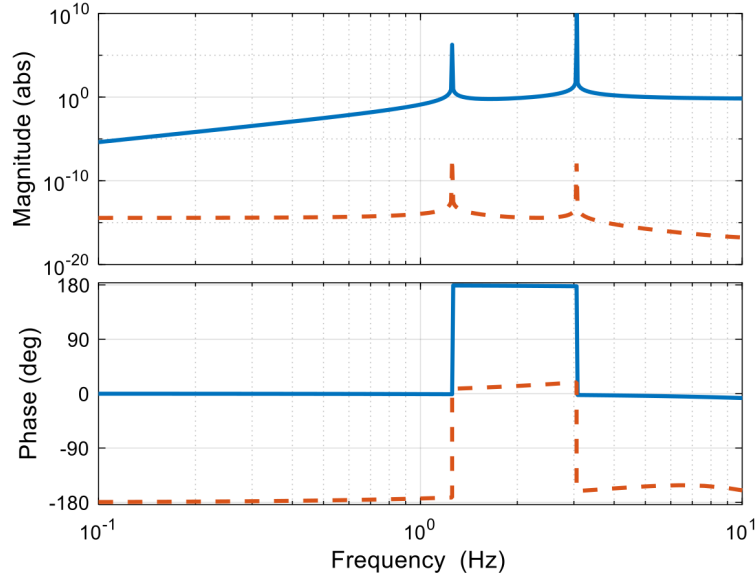


Figure 10. Response of the sensor to translation, $\frac{Y_{\text{new}}}{W_{\text{new}}}$ (blue/bold) and tilt, $\frac{Y_{\text{new}}}{\theta_{\text{new}}}$ (red/dotted).

So it is not a surprise that R increases with increase in link 1 stiffness, since the link will be more firmly attached to the platform and the motion of the platform will affect link 1 more aggressively. Also, a comparison is done based on varying mass of the links. As the mass of link 1 increases, better decoupling is obtained due to an increase in the inertia. Since it is connected to the platform using very low stiff joints, the motion of the platform during tilt is transferred less to the link 2 as compared during translation. A summary of the findings is given in table 3. So, for a better decoupling we have to implement a sensor with joints having very low stiffness, having low L_1/L_2 and high M_1/M_2 ratios.

Table 3. Effect of various parameters on R .

Parameter	Effect on R
Length of Links	Decreases with decrease in L_1/L_2 ratio
Stiffness of Link Joints	Decreases with decrease in k_1/k_2 ratio
Mass of Links	Decreases with increase in M_1/M_2 ratio

4.2 Equilibrated bar configuration

A configuration with equilibrated bar can be also considered instead of the double pendulum configuration mentioned above. The system also has two links and the output is the relative displacements (displacement of point A relative to B) of the two links as shown in figure 12.

A comparison of R between various sensor configurations under the action of translation and tilt, is given in figure 13. The proposed double link sensor is capable of mitigating the TH coupling very efficiently since the ratio, R , is very small as compared to others. The figure also includes that of suspended seismometer method which is an effective one as per figure 5. The performance

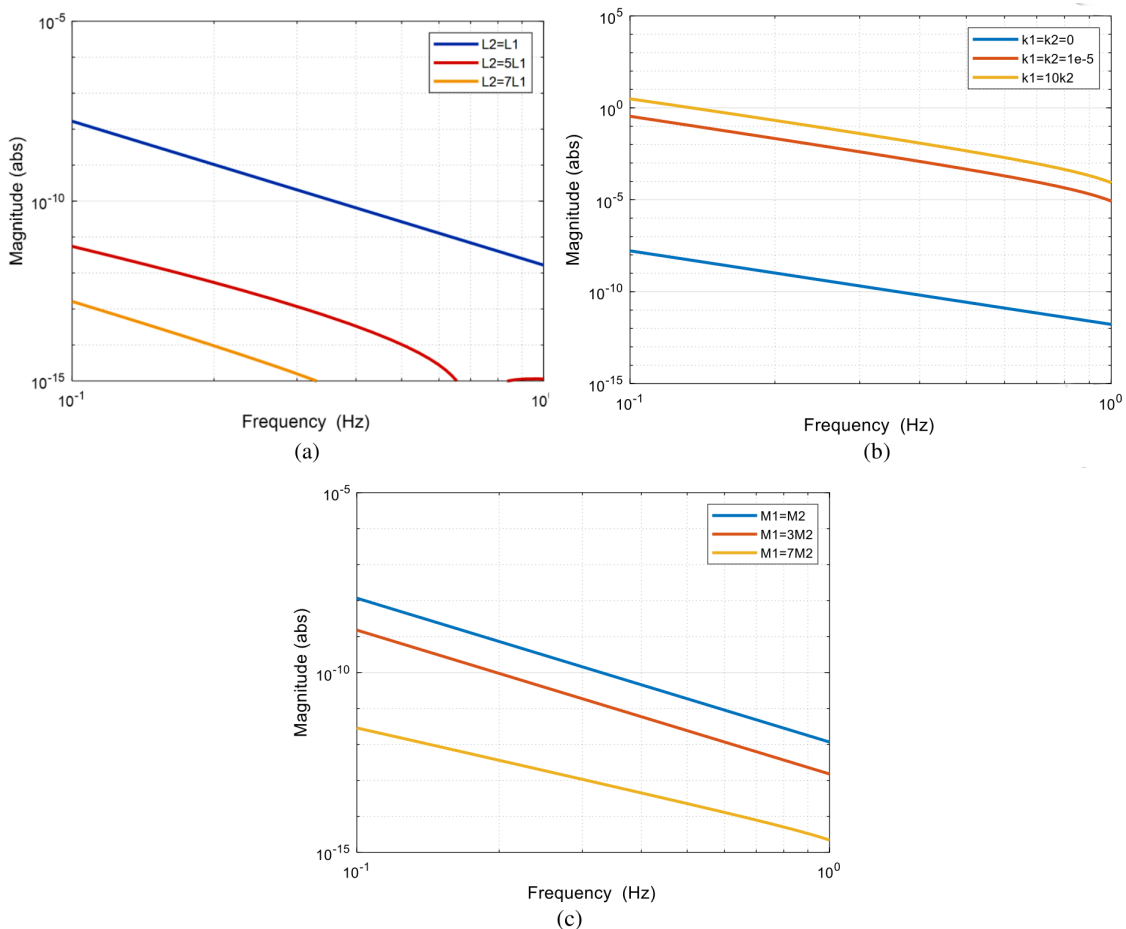


Figure 11. Effect of various sensor parameters on the decoupling efficiency ratio, R . (a) Effect of link lengths, L_1 and L_2 (b) Effect of joint stiffness and (c) Effect of link masses. For a better decoupling we have to implement a sensor with joints having very low stiffness, having low L_1/L_2 and high M_1/M_2 ratios.

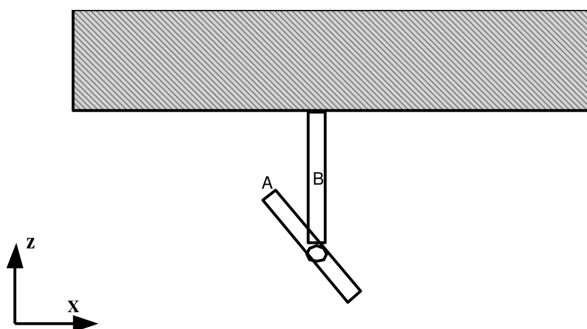


Figure 12. Schematic of the sensor on a platform in equilibrated bar configuration. The sensor has two links with link masses, M_1 and M_2 , fixed on a platform (Shaded). The forces applied for the analysis are the translation in x direction and tilt about y axis. The output of the sensor is the relative displacements of the points A and B .

of equilibrated bar configuration is also satisfactory but at higher frequency it is evident that the performance degrades as compared to the double link configuration.

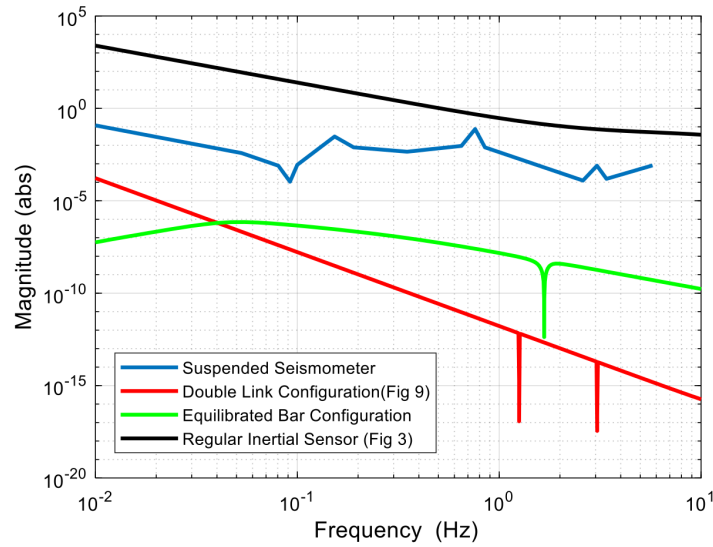


Figure 13. Comparison of decoupling efficiency ratio, R , for various sensor configurations for translation and tilt inputs.

5 Conclusion

A new sensor architecture is presented which is sensitive to translation and negligibly sensitive to tilt thereby mitigating the problem of tilt horizontal coupling when exposed to translation or tilt. The sensor is in the form of a double pendulum hanging from a platform and the measured output is the relative motion between the two links. Simscape models are developed for analysis. The results show the efficiency of the system to handle tilt horizontal coupling and its applicability in Gravitational Wave detectors and systems alike. It is also observed that for a better decoupling we have to implement a sensor with joints having very low stiffness, having low L_1/L_2 and high M_1/M_2 ratios.

Acknowledgments

The authors would like to thank Interreg ERM for funding the ETEST project. The E-TEST project is carried out within the framework of the Interreg V-A Euregio Meuse-Rhine programme, with € 7,5 million from the European Regional Development Fund (ERDF). By investing EU funds in Interreg projects, the European Union is investing directly in economic development, innovation, territorial development, social inclusion and education in the Euregio Meuse-Rhine.

The authors would also like to thank Manipal Institute of technology Manipal Academy of Higher Education Manipal Karnataka India for providing the required support.

Author contribution statement. Vishnu G Nair: Conceptualization, Methodology, Simulation, Investigation, Validation, Writing – original draft preparation. Christophe Collette: Supervision, Writing – review & editing.

References

- [1] P.W. Rodgers, *The response of the horizontal pendulum seismometer to Rayleigh and Love waves, tilt, and free oscillations of the Earth*, *Bull. Seismol. Soc. Am.* **58** (1968) 1385.
- [2] W.K. Lee, M. Celebi, M.I. Todorovska and H. Igel, *Introduction to the special issue on rotational seismology and engineering applications*, *Bull. Seismol. Soc. Am.* **99** (2009) 945.
- [3] S. De Angelis and P. Bodin, *Watching the Wind: Seismic Data Contamination at Long Periods due to Atmospheric Pressure-Field-Induced Tilting*, *Bull. Seismol. Soc. Am.* **102** (2012) 1255.
- [4] B. Lantz, R. Schofield, B. O'Reilly, D.E. Clark and D. DeBra, *Review: Requirements for a ground rotation sensor to improve Advanced LIGO*, *Bull. Seismol. Soc. Am.* **99** (2009) 980.
- [5] K. Venkateswara et al., *Subtracting Tilt from a Horizontal Seismometer Using a Ground-Rotation Sensor*, *Bull. Seismol. Soc. Am.* **107** (2017) 709.
- [6] C. Collette et al., *Review: Inertial sensors for low frequency seismic vibration measurement*, *Bull. Seismol. Soc. Am.* **102** (2012) 1289
- [7] F. Matichard and M. Evans, *Review: Tilt-Free Low-Noise Seismometry*, *Bull. Seismol. Soc. Am.* **105** (2015) 497.
- [8] F. Matichard et al., *Modeling and Experiment of the Suspended Seismometer Concept for Attenuating the Contribution of Tilt Motion in Horizontal Measurements*, *Rev. Sci. Instrum.* **87** (2016) 065002 [[arXiv:1602.01494](https://arxiv.org/abs/1602.01494)].
- [9] https://www.mecal.eu/fileadmin/mecal/downloads/semiconductor_industry/Hummingbird_article.pdf
- [10] W. Hua *Low frequency vibration isolation and Alignment system for advanced LIGO*, Ph.D. Thesis, Stanford University, Stanford, U.S.A. (2005).
- [11] C.M. Mow-Lowry and D. Martynov, *A 6D interferometric inertial isolation system*, *Class. Quant. Grav.* **36** (2019) 245006 [[arXiv:1801.01468](https://arxiv.org/abs/1801.01468)].
- [12] C.C. Speake and D.B. Newell, *The design and application of a novel high-frequency tiltmeter*, *Rev. Sci. Instrum.* **61** (1990) 1500.
- [13] F. Matichard et al., *Seismic isolation of Advanced LIGO: Review of strategy, instrumentation and performance*, *Class. Quant. Grav.* **32** (2015) 185003 [[arXiv:1502.06300](https://arxiv.org/abs/1502.06300)].
- [14] J. Winterflood, Z.B. Zhou, L. Ju and D.G. Blair, *Tilt suppression for ultra-low residual motion vibration isolation in gravitational wave detection*, *Phys. Lett. A* **277** (2000) 143.
- [15] Y. Cheng, J. Winterflood, L. Ju and D.G. Blair, *Tilt sensor and servo control system for gravitational wave detection*, *Class. Quant. Grav.* **19** (2002) 1723.
- [16] A. Sunderland et al., *High performance rotational vibration isolator*, *Rev. Sci. Instrum.* **84** (2013) 105111.
- [17] F. Matichard et al., *Modeling and Experiment of the Suspended Seismometer Concept for Attenuating the Contribution of Tilt Motion in Horizontal Measurements*, *Rev. Sci. Instrum.* **87** (2016) 065002 [[arXiv:1602.01494](https://arxiv.org/abs/1602.01494)].
- [18] P. Knothe, *Tilt attenuation of a seismometer for the measurement of very low frequency seismic signals through suspension*, Ph.D. Thesis, Karlsruher Institut für Technologie, Karlsruhe, Germany (2013).
- [19] A. Marrocchesi, *A prototype for a tilt-free seismometer*, LIGO consortium, Technical Note LIGO-T1500485v1 2015/10/17.

- [20] P. Chawah et al., *A simple pendulum borehole tiltmeter based on a triaxial optical-fibre displacement sensor*, *Geophys. J. Int.* **203** (2015) 1026.
- [21] M. Maggiore et al., *Science Case for the Einstein Telescope*, *JCAP* **03** (2020) 050 [[arXiv:1912.02622](https://arxiv.org/abs/1912.02622)].
- [22] P. Boscariol and D. Richiedei, *Robust point-to-point trajectory planning for nonlinear underactuated systems: Theory and experimental assessment*, *Robot. Comput. Integr. Manuf.* **50** (2017) 50.
- [23] A. Allocca et al., *Picoradiant tiltmeter and direct ground tilt measurements at the Sos Enattos site*, *Eur. Phys. J. Plus* **136** (2021) 1069.